*Published online 27 May 2010*

*Nucleic Acids Research, 2010, Vol. 38, No. 14* ***e148***
*doi:10.1093/nar/gkq436*

# Ratiometric bimolecular beacons for the sensitive detection of RNA in single living cells

**Antony K. Chen[1], Olga Davydenko[2], Mark A. Behlke[3] and Andrew Tsourkas[1,*]**

[1]Department of Bioengineering, [2]Department of Biology, University of Pennsylvania, Philadelphia, PA 19104 and [3]Integrated DNA Technologies Inc., Coralville, IA 52241, USA

Received February 14, 2010; Revised May 4, 2010; Accepted May 7, 2010

## ABSTRACT

**Numerous studies have utilized molecular beacons (MBs) to image RNA expression in living cells; however, there is growing evidence that the sensitivity of RNA detection is significantly hampered by their propensity to emit false-positive signals. To overcome these limitations, we have developed a new RNA imaging probe called ratiometric bimolecular beacon (RBMB), which combines functional elements of both conventional MBs and siRNA. Analogous to MBs, RBMBs elicit a fluorescent reporter signal upon hybridization to complementary RNA. In addition, an siRNA-like double-stranded domain is used to facilitate nuclear export. Accordingly, live-cell fluorescent imaging showed that RBMBs are localized predominantly in the cytoplasm, whereas MBs are sequestered into the nucleus. The retention of RBMBs within the cytoplasmic compartment led to >15-fold reduction in false-positive signals and a significantly higher signal-to-background compared with MBs. The RBMBs were also designed to possess an optically distinct reference fluorophore that remains unquenched regardless of probe confirmation. This reference dye not only provided a means to track RBMB localization, but also allowed single cell measurements of RBMB fluorescence to be corrected for variations in probe delivery. Combined, these attributes enabled RBMBs to exhibit an improved sensitivity for RNA detection in living cells.**

## INTRODUCTION

The ability to image RNA in single living cells has the potential to provide complete spatial and temporal information on gene expression, which is vital to our understanding of the role of RNA in biology and medicine. Currently, the majority of live-cell RNA imaging approaches utilize molecular beacons (MBs) (1), which are antisense oligonucleotides labeled with a fluorophore on one end and a quencher on the other. In the absence of complementary RNA targets, MBs are designed to form a stem-loop structure whereby the fluorophore and the quencher are held in close proximity creating a low fluorescence state. Hybridization with complementary RNA targets results in the separation of the fluorophore and the quencher and fluorescence is restored. The unique ability of MBs to convert target recognition into a detectable fluorescence signal has rendered MBs the probe of choice for studying the expression, distribution and transport of specific RNA molecules in living cells (2–9).

Despite being utilized extensively for live-cell RNA imaging, it has been observed that when MBs are introduced into living cells they can be quickly sequestered into the nucleus where they generate false-positive signals (10–14). We recently showed that false-positive signals could be eliminated simply by retaining MBs within the cytoplasm (10,11), even when nuclease-vulnerable DNA backbones are utilized. Cytoplasmic retention was accomplished via the conjugation of MBs to quantum dots (QD) or NeutrAvidin, which are too large to traverse the nuclear pores. However, while this approach provides an effective means for eliminating false-positive signals, the large size of the MB-conjugate does have some drawbacks. For example, movement of the MB-conjugate within the cytoplasm may be severely restricted (15). Additionally, the QD/NeutrAvidin may sterically hinder the rate of MB-target hybridization. Further, the ability to efficiently deliver large MB-conjugates into the cytoplasm can be a formidable challenge. Clearly, an RNA imaging probe that does not require the incorporation of a macromolecule to prevent nuclear sequestration, and the resulting false-positive signals, would offer many advantages. Here, we show that an RNA imaging probe composed entirely of oligonucleotides can be retained in the cytoplasm by simply combining the functional elements of MBs with structural features of siRNA. This new probe design was based on recent findings that showed siRNA is efficiently exported from the nucleus by exportin (16).

*To whom correspondence should be addressed. Tel: +1 215 898 8167; Fax: +1 215 573 2071; Email: atsourk@seas.upenn.edu

A second optically distinct reference fluorophore that remains unquenched regardless of probe confirmation has also been included in the design of this new RNA imaging probe, which has been aptly named a ratiometric bimolecular beacon (RBMB). The reference fluorophore not only provides a means to track probe localization, but also allows single cell measurements of RBMB fluorescence to be corrected for variations in probe delivery. To demonstrate the benefits of using RBMBs to detect RNA in living cells, the intracellular localization, biostability, functionality and sensitivity were compared with conventional MBs.

## METHODS

### Cell culture

MEF/3T3 cells were cultured in Dulbeco's MEM media supplemented with 1% Penn/Strep, 10% fetal bovine serum (FBS) and incubated in 5% $CO_2$ at 37°C. Both Hela and MCF-7 cells were cultured in Eagle's minimum essential medium with 2 mM L-glutamine and Earle's BSS adjusted to contain 1.5 g/l sodium bicarbonate, 0.1 mM non-essential amino acids, 1 mM sodium pyruvate and 10% FBS in 5% $CO_2$ at 37°C. All cells were obtained from ATCC (Manassas, VA, USA). To generate cells that express Firefly luciferase, cells were infected with adenovirus, H4′ 040CMVffLuciferase (Penn Genomic Center, Philadelphia, PA, USA), at a multiplicity of infection of $10^4$ particles per cell. Infection was carried out 24 h prior to delivery of RBMBs or MBs without any apparent loss of viability. Firefly activity was confirmed by making bioluminescent measurements on a Glomax 20/20 luminometer (Promega) following the administration of SteadyGlo (Promega). For comparison, cells infected with null adenovirus (H5.050CMVEmpty, Penn Genomic Center, Philadelphia, PA, USA) at a multiplicity of infection of $10^4$ particles per cell, were also prepared.

### Synthesis and design of RBMBs and analogous MBs

Antisense Firefly luciferase RBMBs and MBs were designed to hybridize to a targeting sequence (pGL3-Luc 235-252, Promega, Madison, WI, USA) that is not complementary to any known endogenous RNA target in mammalian cells. The RBMB consists of two 2′-*O*-methyl RNA oligonucleotides that are hybridized together. One of the oligonucleotides is labeled with a Cy5 (GE Life Sciences) reporter dye at the 5′ end and has the sequence: /5Cy5/mGmUmCmAmCmCmUm CmAmGmCmGmUmAmAmGmUmGmAmUmGmUm CmGmUmGmAmCmGmAmCmGmGmCmAmGmCm GmUmGmCmAmGmCmUmCmUmU. The second oligonucleotide is labeled with an IRDye® 800 (Licor) reference dye at the 5′ end and an Iowa Black ® RQ-Sp quencher (IDT) at the 3′ end, and has the sequence:/ 5IRD800/mGmAmGmCmUmGmCmAmCmGmCmUm GmCmCmGmUmC/3UAbQSp/. For cytotoxicity assays and studies involving RBMB detection via flow cytometry, the second oligonucleotide was labeled with Alexa488 (Invitrogen) in place of IRDye® 800. To form RBMBs, equal molar ratios of the two oligonucleotides were allowed to hybridize in phosphate buffer (48 mM $K_2HPO_4$, 4.5 mM $KH_2PO_4$, 14 mM $NaH_2PO_4$), pH 7.2 at room temperature overnight. The resulting RBMBs were then purified from single-stranded oligonucleotides on a Superdex 30 prep grade column (GE healthcare) and concentrated on Microcon YM-10 centrifugal devices (10 000 MW cutoff; Millipore). The final concentration of the RBMBs was determined spectrophotometrically using a Cary 100 spectrophotometer (Varian). An analogous 2′-*O*-methyl RNA MB was synthesized with the sequence: /5Cy5/mGmUmCmAmCmCmUmCmAmGm CmGmUmAmAmGmUmGmAmUmGmUmCmG/iboT/ mGmAmC/3IAbRQSp/ (17). A luciferase RNA target with the sequence: UGGACAUCACUUACGCUG AGUA was also synthesized. All oligonucleotides were synthesized by Integrated DNA Technologies (IDT).

### Optical properties of RBMB

The emission profile of each RBMB was acquired on the FluoroMax-3 spectrofluorometer (Horiba Jobin Yvon) by setting the excitation wavelength to 647 nm for Cy5 and 780 nm for IRDye®800. Emission scans from 655 to 800 nm and from 790 to 850 nm were performed, respectively. These experiments were carried out in phosphate buffer, pH 7.2 using 250 nM RBMB in the presence or absence of 2.5 μM complementary RNA target.

### Synthesis of fluorescently labeled dextran

Aminodextran (MW: 10 kDa, Invitrogen) was dissolved in 50 mM sodium borate buffer (pH 8) at a concentration of 10 mg/ml and reacted with 2.5 mM IRDye®800-NHS ester (Li-Cor) at a dye to dextran molar ratio of 2.5 : 1. The fluorescently labeled dextrans were purified on NAP-5 gel chromatography columns (Amersham Biosciences) in phosphate buffer, pH 7.2. The concentration of the IRDye®800 fluorophore was determined spectrophotometrically.

### Cellular delivery of RBMBs and MBs

Microporation was performed with an OneDrop MicroPorator (MP-100, BTX Harvard Apparatus) as per manufacturer's protocol. Specifically, cells were seeded in T-25 flasks in DMEM-FBS with no phenol red and no antibiotics 1 day prior to microporation. Before microporation, the cells were trypsinized, pelleted and re-suspended in media without phenol red and antibiotics, pelleted again, washed with 1× PBS, and re-suspended in re-suspension buffer R (BTX Harvard Apparatus) at a concentration of 120 000 cells per 11 μl. To deliver MBs into the cells, 1 μl of sample containing MBs and IRDye800-labeled dextran were added to the cells such that the final MB concentration and Alexa750-labeled dextran were 5 and 10 μM, respectively. To deliver RBMBs into cells, 1 μl of RBMBs were added to the cells such that the final concentration of RBMBs was also 5 μM. Cells (10μl, i.e. 100 000 cells) incubated in the presence of the probes were then microporated at 1500 V with three pulses of 10 ms width for MEF-3T3 cells, at 990 V with a single pulse of 50 ms width for MCF-7 cells and at 1005 V with two pulses of 35 ms width for HeLa

cells. Following microporation, the cells were washed once in 1× PBS and re-suspended in the DMEM (without phenol red and supplemented with 10% FBS) and then seeded into the 8-well Lab-Tek Chambered Coverglass (155409, Nalge Nunc) or Glass bottom Dish (Willco Wells). Fluorescence images were acquired ~10 min (i.e. immediately after cell seeding), 1, 2, 3, 4, 5 and 24 h after microporation.

### Cytotoxicity assay

The effect of microporation on the viability of MEF-3T3, MCF-7 and HeLa cells was assessed via an MTT assay (ATCC) according to the manufacturer's instructions. Absorbances (570 nm) were measured spectrophotometrically. Viability of cells was determined by dividing the absorbance measurements of the electroporated cells by the absorbance of cells that were not electroporated (0 V).

### Transfection efficiency

Following microporation of MEF-3T3, MCF-7 or HeLa cells in the presence of RBMBs with Alexa488 as the reference dye, the cells were washed once in PBS and analyzed on a guava excite flow cytometer fitted with a 488 nm excitation laser. Flow cytometry data was analyzed with FLOWJO (Version 7.2.2; Tree Star, Ashland, OR, USA). Fluorescence signal intensity was defined as the mean intensity of cells lying within a predefined gate. The appropriate gate was defined on an FSC versus SSC dot plot of cells that were not electroporated (0 V).

### Fluorescent microscopy

All microscopy images were performed on an Olympus I× 81 motorized inverted fluorescence microscope equipped with a back-illuminated EMCCD camera (Andor), an X-cite 120 excitation source (EXFO) and sutter excitation and emission filter wheels. Images of Cy5 and IRDye® 800 were acquired using the filter sets (HQ620/60, HQ700/75, Q660LP) and (HQ710/75, HQ810/90, Q750LP) (Chroma). A LUC PLAN FLN 40× objective (NA 0.9) was used for all imaging studies. Results were analyzed with NIH Image J.

### Ratiometric analysis

*Water-in-oil emulsions*. Emulsions containing MBs and fluorescently labeled dextrans or RBMBs were prepared as described previously (18). For each water-in-oil bubble, two images were acquired, one corresponding to the reporter dye (i.e. Cy5) and the other to the reference dye (i.e. IRDye®800) on the dextran or RBMB. A region of interest (ROI) was drawn around each bubble, and the total fluorescent intensity was measured in each image. Similarly, the total fluorescence intensity from an ROI of equal size drawn around a 'background' region was also measured for each image. The background subtracted fluorescence measurement for the reporter and the reference moiety was then calculated. The fluorescence ratio, $F_{rep}/F_{ref}$, was then calculated by dividing the background subtracted MB fluorescence by the background subtracted reference fluorescence.

*Single cell analysis*. Ratiometric analysis was performed on images of the cells using a method analogous to that used for water-in-oil emulsions, except the ROI was drawn around individual cells.

### Analysis of RBMB/MB nonspecific opening

Procedures to determine the extent of MB non-specific opening in living cells was described previously (12). In brief, the fluorescence ratio, $F_{rep}/F_{ref}$, was first determined for cell and microemulsion samples as described earlier. Then, the percent of MBs opened was calculated as the follows:

$$\%\ \text{MBs Opened} = \frac{R_{\text{CELL}} - R_{\text{BUBBLE, CLOSED}}}{R_{\text{BUBBLE, OPENED}} - R_{\text{BUBBLE, CLOSED}}}, \quad (1)$$

where $R_{\text{CELL}}$ is the fluorescence ratio, $F_{rep}/F_{ref}$, in living cells, and $R_{\text{BUBBLES, CLOSED}}$ and $R_{\text{BUBBLES, OPENED}}$ refer to the fluorescent ratio, $F_{rep}/F_{ref}$, for the unhybridized (fully quenched) and fully hybridized MBs, respectively, from the water-in-oil emulsions. The same study was also performed to quantify the extent of non-specific RBMB opening in living cells.

### Functionality assay

Aqueous samples containing 100 μM synthetic luciferase RNA targets in phosphate buffer, pH 7.2 were microinjected into cells containing MBs or RBMBs using a Femtojet and Injectman NI 2 (Eppendorf) microinjection system fitted with Femtotips I (Eppendorf). The targets were injected into cells at 24 h post-microporation. Fluorescent images of each cell were acquired immediately before and shortly after injection.

### Analysis of RBMB and MB Hybridization signal

In practice, MBs that are in a hairpin conformation still emit a low fluorescence background signal due to incomplete quenching of the fluorophore by the quencher. This means that the total MB signal emitted by a cell is the sum of the MB background signal and MB enhancement signal (i.e. due to hybridization and/or false-positive signals). Assuming the fluorescence ratio $F_{rep}/F_{ref}$ is the same in aqueous bubbles and in living cells (18), the contribution of MB background fluorescence to the total signal in cells can be calculated by the product of $F_{ref}$ and the fluorescent ratio of the aqueous bubble ($R_{\text{BUBBLES, CLOSED}}$). The MB enhancement signal can then be determined as the difference between the total integrated MB signal ($\text{MB}_{\text{CELL}}$) and the MB background signal in cells, as follows:

$$\text{MB signal enhancement} = \text{MB}_{\text{CELL}} - \text{REF}_{\text{CELL}} \times R_{\text{BUBBLE, CLOSED}}. \quad (2)$$

Equation (2) was also applied to quantify the extent of RBMB and MB hybridization in living cells.

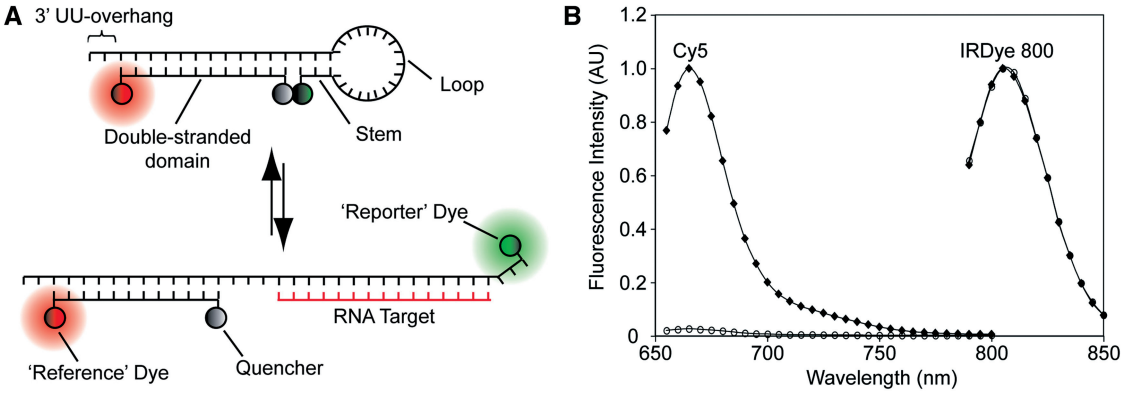


**Figure 1.** Schematic and fluorescent emission spectra of RBMBs. (**A**) RBMBs are hairpin-forming oligonucleotide probes that are labeled with a reporter fluorophore, reference fluorophore and quencher. In the absence of complementary targets, the reporter fluorophore and quencher are held in close proximity resulting a low fluorescence state. In the presence of target, the reporter fluorophore and quencher are separated and fluorescence is restored. The reference fluorophore remains unquenched regardless of the RBMB conformation. The long double-stranded domain with a UU-overhang was designed to mimic the structure of siRNA and is used to drive nuclear export. (**B**) Emission spectra of an RBMB (Cy5 reporter, Iowa Black RQ quencher, and an IRdye®800 reference dye) in the absence (open circle) and presence (filled diamond) of excess complementary RNA targets.

## RESULTS AND DISCUSSION

### Design and characteristics of RBMBs

RBMBs are composed of two hybridized oligonucleotides (Figure 1A). One of the oligonucleotides forms a stem loop structure with one arm of the stem being significantly longer than the other. The shorter stem is labeled with a 'reporter' dye. The longer stem is complementary to a second oligonucleotide that is labeled with a 'reference' dye at one end and a quencher at the other, such that formation of the bimolecular construct brings the quencher into close proximity to the 'reporter' dye, while the optically distinct 'reference' dye is held at the far end of the hybrid. The double-stranded domain of the RBMB is designed to be of sufficient length such that the reference dye does not interact with the quencher and the hybrid melting temperature is well above physiological temperature, to ensure that the hybrid does not dissociate in cells. A 2-base (UU) single-stranded overhang is included at the 3′ end of the duplex to resemble the structure of siRNA. It has previously been shown that siRNA is efficiently exported from the nucleus by exportin (16), therefore, it was hypothesized that incorporation of siRNA-like elements into the RBMB design would result in cytoplasmic localization.

In this study, all RBMBs were synthesized with 2′-*O*-methyl RNA backbones, a Cy5 reporter dye and an Iowa Black RQ quencher. IRDye®800 was used as the reference dye. The emission spectra of RBMBs in the presence and absence complementary RNA targets are shown in Figure 1B. In the absence of target, the fluorescence emission of the Cy5 reporter dye was efficiently quenched, consistent with RBMBs assuming a hairpin conformation with the reporter dye and quencher being held in close proximity. Following the addition of complementary nucleic acid targets, there was >35-fold increase in reporter fluorescence. The mechanism responsible for the restoration of fluorescence is similar to that of conventional MBs, with RNA hybridization driving the separation of the reporter dye and quencher. Since the distance between the reference dye, IRDye®800, and quencher is unaffected by RBMB hybridization its fluorescence remained unchanged.

### Intracellular delivery, localization and biostability of RBMBs

RBMBs were delivered into living cells via microporation. Microporation is a microliter-volume electroporation process that exhibits a reduction in the many harmful events often associated with electroporation, including heat generation, metal ion dissolution, pH variation and oxide formation (www.microporator.com). Microporation exhibited a delivery efficiency of >98% for MEF/3T3, HeLa and MCF-7 cells (Supplementary Figure S1). To specifically test the effect of microporation on cell viability, an MTT cell proliferation assay was performed on each cell line. The viability was 97 ± 10%, 93 ± 11% and 94 ± 2% for MEF/3T3, HeLa and MCF-7 cells, respectively. These results suggest that microporation provides a very effective method for the delivery of RBMBs into living cells.

Following the delivery of RBMBs (or analogous MBs) into MEF/3T3, HeLa or MCF-7 cells, the intracellular distribution was assessed by fluorescence microscopy. The targeting domain of both probes was chosen such that it was not complementary to any known endogenous RNAs. Therefore, it was expected that both probes would remain in a quenched state unless opened due to non-specific interactions and/or nuclease degradation. Approximately 10 min after microporation, the unquenched reference dye revealed that the RBMBs were distributed relatively uniformly throughout the cytoplasm and nucleus with, perhaps, a slight preference for the cytoplasm (Figure 2A). By 5 h the RBMBs were predominantly localized within the cytoplasm. After 24 h, the RBMBs were still predominantly localized within the

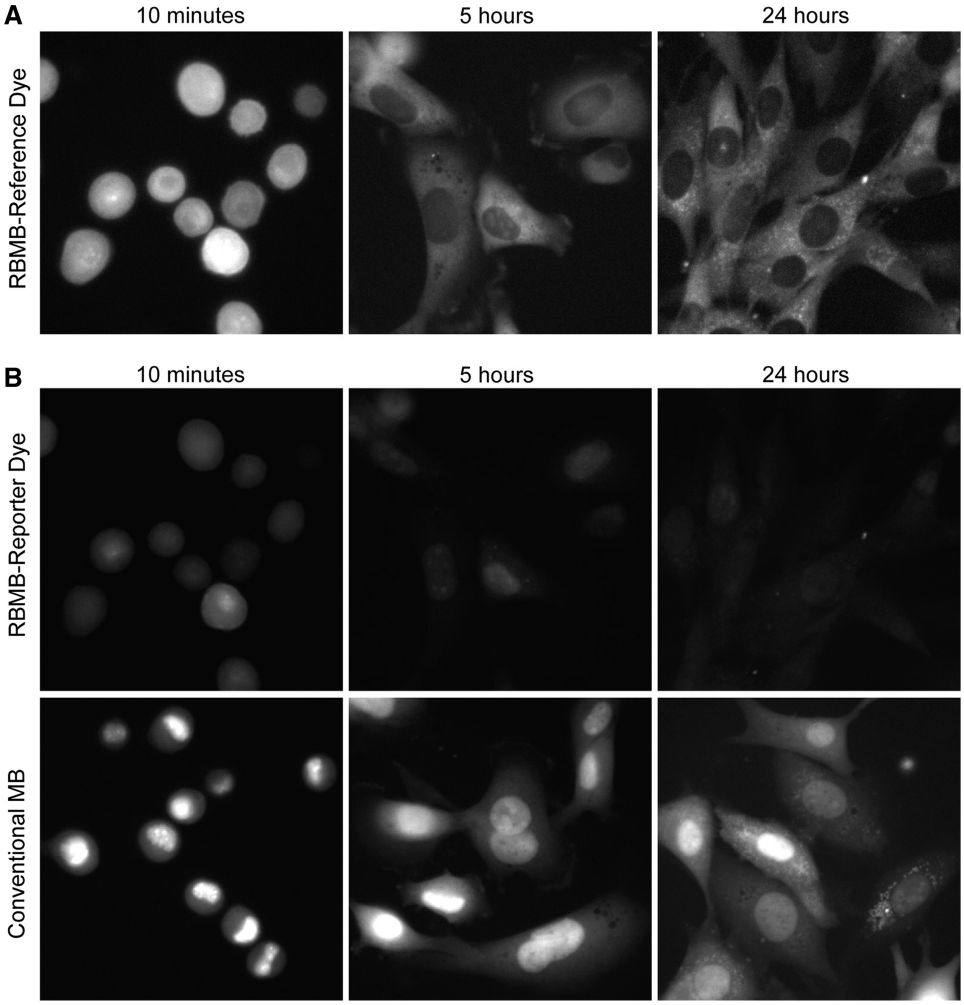


**Figure 2.** Fluorescent images of MEF/3T3 cells at various times after microporation with non-sense MBs or RBMBs. (**A**) Images of the RBMB reference dye. (**B**) Images of the RBMB (top row) and conventional MB (bottom row) reporter dye. Representative fluorescence images are shown immediately following microporation (i.e. 10 min) as well as 5 and 24 h after microporation. The contrast for all images in (B) was adjusted simultaneously.

cytoplasm; however, there was a small amount of punctate fluorescence, presumably due to some uptake by lysosomes. Overall, these results suggest that incorporation of the siRNA-like structural elements into the RBMB design allowed for the efficient export of the RBMBs from the nucleus.

Fluorescent images of the RBMB reporter dye revealed that RBMB reporter fluorescence was well quenched for at least 24 h (Figure 2B, top row). There was a faint fluorescent signal that could be observed in the nucleus of some cells, but overall the fluorescent signal within the cells was barely above background, suggesting very effective quenching of the Cy5 reporter dye. Conversely, conventional MBs elicited a bright fluorescent signal within the nucleus within 10 min of being microporated into cells (Figure 2B, bottom row). Only a faint fluorescent signal was observed in the cytoplasm. This pattern remained similar for at least 24 h, although the overall fluorescent intensity of the MBs did appear to increase with time. These results suggest that while RBMBs exhibit very little non-specific opening, conventional MBs exhibit a significant extent of non-specific opening, primarily within the nucleus of living cells, which is consistent with our previous findings (10–12).

To quantify the extent of RBMB nonspecific opening, the fluorescent ratio (i.e. total integrated reporter fluorescence/total integrated reference fluorescence, $F_{rep}/F_{ref}$), was compared with fluorescence microscopy measurements of the same RBMB samples prior to intracellular delivery. Specifically, water-in-oil emulsions were prepared with the RBMB samples in the absence and presence of target, representing 0 and 100% opening of the RBMBs, respectively (12). Images of the fluorescent bubbles were then acquired directly on the microscope and the ratio, $F_{rep}/F_{ref}$, was calculated. Using these extracellular measurements as standards, the percent of open RBMBs within living cells was determined. A similar analysis was conducted with conventional MBs in the presence of dextran (10 kDa) labeled with IRDye® 800.

Interestingly, ratiometric analysis revealed that <1% of the RBMBs were opened non-specifically in MEF/3T3 cells 5 h after microporation. Further, only 1.2% of the

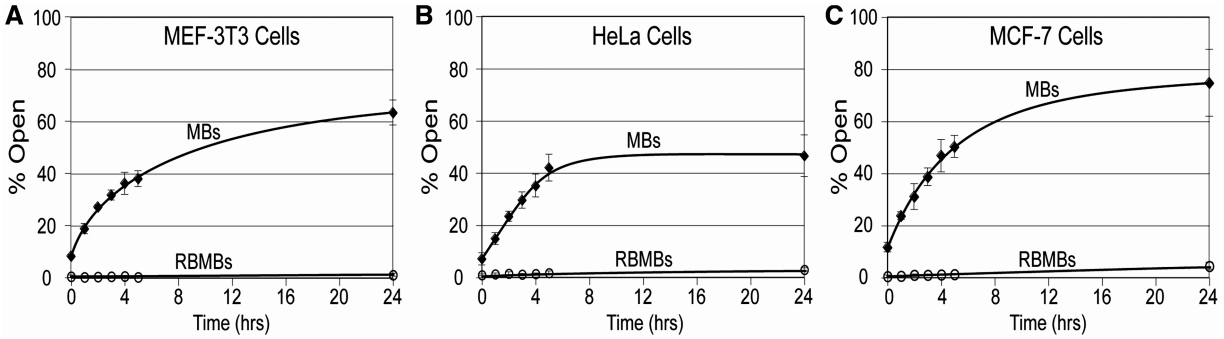


**Figure 3.** Quantitative analysis of non-specific MB and RBMB opening in living cells. Non-sense MBs (filled diamond) and RBMBs (open circle) were microporated into (**A**) MEF/3T3, (**B**) HeLa and (**C**) MCF-7 cells and the percent non-specific opening was quantified over the course of 24 h. Each data point represents the mean and SD from at least 50 cells.

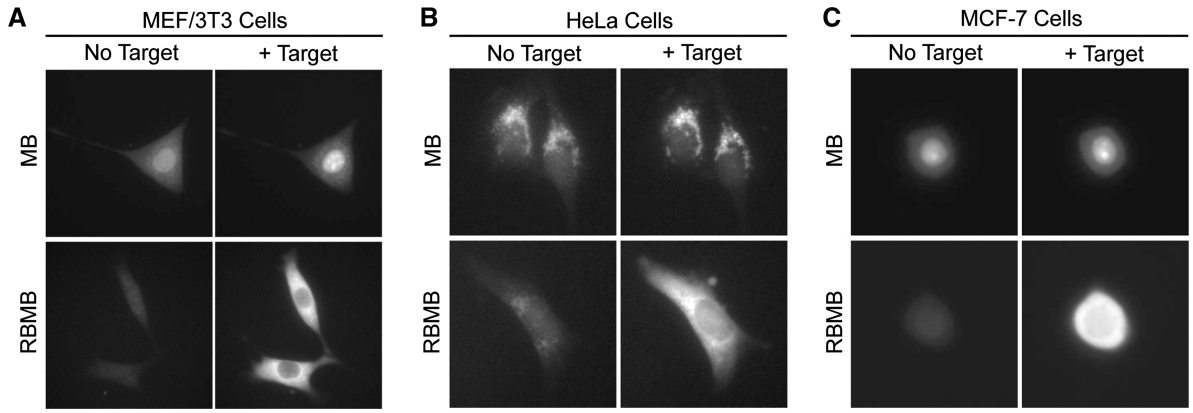


**Figure 4.** Functional analysis of MBs and RBMBs in living cells. Twenty-four hours following the microporation of MBs or RBMBs into (**A**) MEF/3T3, (**B**) HeLa and (**C**) MCF-7 cells, excess complementary RNA targets were microinjected into the cytoplasm. Fluorescent images of the cells were acquired immediately before and several minutes after microinjection. Representative fluorescent images are shown.

RBMBs were open after 24 h (Figure 3A). In contrast, the MBs actually exhibited a very significant amount of non-specific opening following microporation (Figure 3A). Approximately 8% of the MBs were opened within 10 min following microporation into MEF/3T3 cells and by 24 h nearly 63% of the MBs were open. This is consistent with our previous findings (12). Similar results were obtained when RBMBs and MBs were introduced into HeLa and MCF-7 cells (Figure 3B and C). Overall, these results demonstrate that RBMBs are far more resistant to non-specific opening in living cells than conventional MBs.

### Functional analysis of RBMBs in living cells

To assess the functionality of RBMBs and MBs following delivery into live cells, excess complementary RNA targets were microinjected into the cytosol of single cells 24 h after microporation. Fluorescent images were acquired immediately before and shortly after microinjection. Representative images of MEF/3T3 cells are shown in Figure 4A. While cells with MBs exhibited little to no enhancement in fluorescence following injection of nucleic acid targets, cells with RBMBs exhibited a substantial enhancement in fluorescence. Quantitative analysis of cellular fluorescence before and after the injection of RNA targets revealed that RBMBs exhibited a signal enhancement (i.e. signal-to-background, S:B) of $9.0 \pm 2.4$. In contrast, conventional MBs exhibited a S:B of only $1.12 \pm 0.07$. Similar observations were made for HeLa and MCF-7 cells (Figure 4B and C). Specifically, RBMBs exhibited a S:B of $9.9 \pm 3.2$ and $15.3 \pm 3.3$ in Hela and MCF-7 cells, respectively, while conventional MBs exhibited a S:B of less than 1.25 for both cell lines. These results suggest that far more RBMBs are functionally active after 24 h compared with MBs, which is not surprising considering their much lower extent of non-specific opening. Overall, these results suggest that RBMBs may potentially be utilized for the long-term monitoring of gene expression.

### Sensitivity of RBMBs for intracellular RNA detection

To confirm that RBMBs could be used to detect gene expression in single living cells, antisense luciferase RBMBs were delivered into MEF/3T3 cells that express Firefly luciferase (luc+). Cells that did not express Firefly luciferase (luc−) were used as a negative control. Figure 5A shows the fluorescence intensity histograms of cells that were imaged 3–5 h after microporation.

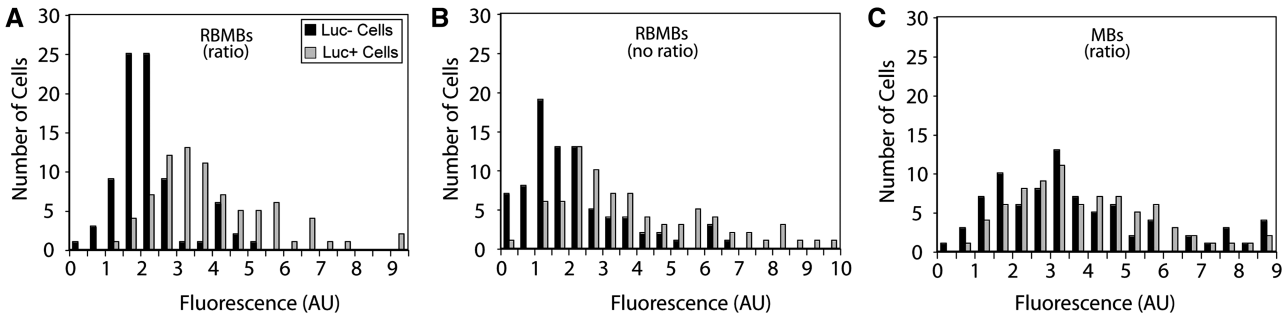


**Figure 5.** Intracellular RNA detection using MBs and RBMBs. (**A**) Luc+ and luc− MEF/3T3 cells were microporated in the presence of anti-sense luciferase RBMBs. Fluorescence measurements of single living cells were acquired 3–5 h after microporation and fluorescence intensity histograms were constructed. Measurements of the reference dye were used to correct for cell-to-cell variations in reporter fluorescence owing to inhomogeneities in probe delivery. (**B**) Fluorescence intensity histograms of RBMB fluorescence in luc+ and luc− cells, for same cells analyzed in (A), but fluorescence measurements were not adjusted for inhomogeneities in probe delivery. (**C**) Fluorescence intensity histograms of MB fluorescence in luc+ and luc− cells. MBs were microporated into MEF/3T3 cells in the presence of fluorescently-labeled (IRDye®800) dextran. The IRDye®800 signal was used to correct for cell-to-cell variations in reporter fluorescence owing to inhomogeneities in probe delivery. At least 80 cells were analyzed for each experimental condition.

The mean fluorescent intensity was 150% higher in luc+ cells than in the luc− cells ($P < 0.0001$). It should be noted that measurements of the reference dye were used to correct for cell-to-cell variations in reporter fluorescence owing to inhomogeneities in probe delivery. When ratiometric imaging approaches were not applied, the mean fluorescent intensity was only 64% higher in luc+ cells than in luc− cells ($P < 0.001$) (Figure 5B). Therefore, ratiometric measurements led to >2.3-fold improvement in sensitivity. Even when ratiometric imaging was employed, the total enhancement in fluorescence in luc+ cells was only a small fraction of the full dynamic range of RBMBs. Although this likely reflects a higher number of RBMBs than RNA in cells, it could also, in part, be a consequence of incomplete RBMB hybridization with target RNA, due to interference from RNA-binding proteins or RNA secondary structure. It has previously been shown that the extent of RNA binding in living cells is highly dependent on the selection of target sequences and their accessibility (19).

Regardless of the specific RNA target sequence selected, it was expected that RBMBs would exhibit an improvement in the sensitivity of RNA detection compared with analogous MBs. To confirm this hypothesis, antisense luciferase MBs were delivered into luc+ and luc− MEF/3T3 cells and cellular fluorescence was quantified (Figure 5C). Results indicated that MBs exhibited similar mean fluorescence intensities in both luc+ and luc− cells ($P = 0.476$). Presumably, the non-specific, false-positive signals observed in the nucleus hampered the ability of MBs to detect target RNA in this study. Overall, these results clearly underline the advantages of RBMBs for live-cell RNA detection.

In summary, we developed a new RNA imaging probe, RBMB, that exhibits high resistance to non-specific opening, high sensitivity for RNA detection, and prolonged functionality in living cells. Nuclear sequestration and false-positive signals were avoided by simply incorporating a structural element that resembles siRNA into the probe design. Further, incorporation of an unquenched, optically distinct reference dye allowed single cell measurements of RBMB fluorescence to be corrected for variations in probe delivery. Combined, these attributes enabled RBMBs to detect lower levels of RNA expression than could be detected by conventional MBs. It is envisioned that the improved sensitivity of RBMBs will allow live cell RNA imaging approaches to be utilized for a much wider range of applications than previously possible.

## SUPPLEMENTARY DATA

Supplementary Data are available at NAR Online.

## FUNDING

Funding for open access charge: National Institute of Health (NCI) R21 CA116102 and R21 CA125088, the National Science Foundation BES-0616031 and the American Cancer Society RSG-07-005-01.

*Conflict of interest statement*. Dr Mark Behlke is employed by IDT which offers oligonucleotides for sale similar to some of the compounds described in the manuscript. IDT is, however, not a publicly traded company and he personally does not own any shares/equity in IDT.

## REFERENCES

1. Tyagi,S. and Kramer,F.R. (1996) Molecular beacons: probes that fluoresce upon hybridization. *Nat. Biotechnol.*, **14**, 303–308.
2. Bratu,D.P., Cha,B.J., Mhlanga,M.M., Kramer,F.R. and Tyagi,S. (2003) Visualizing the distribution and transport of mRNAs in living cells. *Proc. Natl Acad. Sci. USA*, **100**, 13308–13313.
3. Drake,T.J., Medley,C.D., Sen,A., Rogers,R.J. and Tan,W. (2005) Stochasticity of manganese superoxide dismutase mRNA expression in breast carcinoma cells by molecular beacon imaging. *Chembiochem*, **6**, 2041–2047.
4. Nitin,N. and Bao,G. (2008) NLS peptide conjugated molecular beacons for visualizing nuclear RNA in living cells. *Bioconjug. Chem.*, **19**, 2205–2211.
5. Rhee,W.J. and Bao,G. (2009) Simultaneous detection of mRNA and protein stem cell markers in live cells. *BMC Biotechnol.*, **9**, 30.

6. Santangelo,P.J., Nix,B., Tsourkas,A. and Bao,G. (2004) Dual FRET molecular beacons for mRNA detection in living cells. *Nucleic Acids Res.*, **32**, e57.
7. Tyagi,S. and Alsmadi,O. (2004) Imaging native beta-actin mRNA in motile fibroblasts. *Biophys. J.*, **87**, 4153–4162.
8. Yeh,H.Y., Yates,M.V., Mulchandani,A. and Chen,W. (2008) Visualizing the dynamics of viral replication in living cells via Tat peptide delivery of nuclease-resistant molecular beacons. *Proc. Natl Acad. Sci. USA*, **105**, 17522–17525.
9. Bao,G., Rhee,W.J. and Tsourkas,A. (2009) Fluorescent probes for live-cell RNA detection. *Annu. Rev. Biomed. Eng.*, **11**, 25–47.
10. Chen,A.K., Behlke,M.A. and Tsourkas,A. (2007) Avoiding false-positive signals with nuclease-vulnerable molecular beacons in single living cells. *Nucleic Acids Res.*, **35**, e105.
11. Chen,A.K., Behlke,M.A. and Tsourkas,A. (2008) Efficient cytosolic delivery of molecular beacon conjugates and flow cytometric analysis of target RNA. *Nucleic Acids Res.*, **36**, e69.
12. Chen,A.K., Behlke,M.A. and Tsourkas,A. (2009) Sub-cellular trafficking and functionality of 2′-O-methyl and 2′-O-methyl-phosphorothioate molecular beacons. *Nucleic Acids Res.*, **37**, e149.
13. Mhlanga,M.M., Vargas,D.Y., Fung,C.W., Kramer,F.R. and Tyagi,S. (2005) tRNA-linked molecular beacons for imaging mRNAs in the cytoplasm of living cells. *Nucleic Acids Res.*, **33**, 1902–1912.
14. Molenaar,C., Marras,S.A., Slats,J.C., Truffert,J.C., Lemaitre,M., Raap,A.K., Dirks,R.W. and Tanke,H.J. (2001) Linear 2′ O-Methyl RNA probes for the visualization of RNA in living cells. *Nucleic Acids Res.*, **29**, e89.
15. Seksek,O., Biwersi,J. and Verkman,A.S. (1997) Translational diffusion of macromolecule-sized solutes in cytoplasm and nucleus. *J. Cell Biol.*, **138**, 131–142.
16. Ohrt,T., Merkle,D., Birkenfeld,K., Echeverri,C.J. and Schwille,P. (2006) In situ fluorescence analysis demonstrates active siRNA exclusion from the nucleus by Exportin 5. *Nucleic Acids Res.*, **34**, 1369–1380.
17. Tsourkas,A., Behlke,M.A. and Bao,G. (2003) Hybridization of 2′-O-methyl and 2′-deoxy molecular beacons to RNA and DNA targets. *Nucleic Acids Res.*, **31**, 5168–5174.
18. Chen,A.K., Cheng,Z., Behlke,M.A. and Tsourkas,A. (2008) Assessing the sensitivity of commercially available fluorophores to the intracellular environment. *Anal. Chem.*, **80**, 7437–7444.
19. Rhee,W.J., Santangelo,P.J., Jo,H. and Bao,G. (2008) Target accessibility and signal specificity in live-cell detection of BMP-4 mRNA using molecular beacons. *Nucleic Acids Res.*, **36**, e30.